0026-895X/11/8002-267–280$25.00
MOLECULAR PHARMACOLOGY
Vol. 80, No. 2
70243/3701691
Mol Pharmacol 80:267–280, 2011
Printed in U.S.A.

Structural and Functional Analysis of Two New Positive Allosteric Modulators of GluA2 Desensitization and Deactivation[S]

David E. Timm, Morris Benveniste, Autumn M. Weeks, Eric S. Nisenbaum, and Kathryn M. Partin

Department of Biomedical Sciences, Division of Neuroscience, Colorado State University, Fort Collins, Colorado (A.M.W., K.M.P.); Discovery Chemistry Research & Technologies and Neuroscience Discovery Research, Lilly Research Laboratories, Eli Lilly and Company, Indianapolis, Indiana (D.E.T., E.S.N.); and Neuroscience Institute, Morehouse School of Medicine, Atlanta, Georgia (M.B.)

Received November 30, 2010; accepted May 4, 2011

ABSTRACT

At the dimer interface of the extracellular ligand-binding domain of α-amino-3-hydroxy-5-methylisoxazole-4-propionic acid (AMPA) receptors a hydrophilic pocket is formed that is known to interact with two classes of positive allosteric modulators, represented by cyclothiazide and the ampakine 2*H*,3*H*,6a*H*-pyrrolidino(2,1–3′,2′)1,3-oxazino(6′,5′-5,4)benzo(*e*)1,4-dioxan-10-one (CX614). Here, we present structural and functional data on two new positive allosteric modulators of AMPA receptors, phenyl-1,4-bis-alkylsulfonamide (CMPDA) and phenyl-1,4-bis-carboxythiophene (CMPDB). Crystallographic data show that these compounds bind within the modulator-binding pocket and that substituents of each compound overlap with distinct moieties of cyclothiazide and CX614. The goals of the present study were to determine 1) the degree of modulation by CMPDA and CMPDB of AMPA receptor deactivation and desensitization; 2) whether these compounds are splice isoform-selective; and 3) whether predictions of mechanism of action could be inferred by comparing molecular interactions between the ligand-binding domain and each compound with those of cyclothiazide and CX614. CMPDB was found to be more isoform-selective than would be predicted from initial binding assays. It is noteworthy that these new compounds are both more potent and more effective and may be more clinically relevant than the AMPA receptor modulators described previously.

Introduction

α-Amino-3-hydroxy-5-methylisoxazole-4-propionic acid (AMPA) receptors mediate the initial peak of excitatory postsynaptic potentials and are critical for the strengthening and weakening of synapses that underlie the cellular basis of learning and memory. Positive allosteric modulators of AMPA receptors act by enhancing normal AMPA receptor activity to mimic long-term potentiation (Stäubli et al., 1994a) and prolong open-channel time by slowing or preventing channel closure (Vyklicky et al., 1991; Yamada and Rothman, 1992; Arai et al., 1996a; Partin et al., 1996; Suppiramaniam et al., 2001). Slowing the termination of a glutamate-evoked response enhances excitatory postsynaptic potentials by increasing ion flux through AMPA receptor channels.

Initial studies indicated that potentiating AMPA receptors could alleviate cognitive deficits (Staubli et al., 1994b; Arai et al., 1996b). Currently developed compounds such as the benzamides improve normal cognitive function and cognitive function impaired by aging or schizophrenia (Ingvar et al., 1997; Goff et al., 2001). However, in animal models or human studies, several of these compounds either were not effective or exhibited adverse side effects, demonstrating the challenge to discover compounds that are both effective and tol-

This work was supported by the National Institutes of Health National Institute of Mental Health [2R01-MH064700-06A2]; and the National Institutes of Health National Institute of Neurological Disorders and Stroke [S11-NS055883].

Article, publication date, and citation information can be found at http://molpharm.aspetjournals.org.

doi:10.1124/mol.110.070243.

[S] The online version of this article (available at http://molpharm.aspetjournals.org) contains supplemental material.

ABBREVIATIONS: AMPA, α-amino-3-hydroxy-5-methyl-4-isoxazole propionic acid; CMPDA, phenyl-1,4-bis-alkylsulfonamide; CMPDB, phenyl-1,4-bis-carboxythiophene; Deact, deactivation; Des, desensitization; CTZ, cyclothiazide; CX614, 2H,3H,6aH-pyrrolidino(2,1-3′,2′)1,3-oxazino(6′,5′-5,4)benzo(*e*)1,4-dioxan-10-one; LBC (ligand-binding core), DMSO, dimethyl sulfoxide; WT, wild type; CC, closed clamshell; OC, open clamshell; i, flip; o, flop; HEK, human embryonic kidney; FLIPR, fluorometric imaging plate reader; BAPTA, 1,2-bis(2-aminophenoxy)ethane-*N*,*N*,*N*′,*N*′-tetraacetic acid; PEG, polyethylene glycol; LY404187, *N*-[2-(4′-cyanobiphenyl-4-yl)propyl]propane-2-sulfonamide; CX546, 2,3-dihydro-1,4-benzodioxin-7-yl-(1-piperidyl)methanone; CX516, 6-(piperidin-1-ylcarbonyl)quinoxaline.

erated (Ward et al., 2010a). Reduced glutamatergic signaling is involved in Alzheimer's disease, schizophrenia, attention-deficit/hyperactivity disorder, narcolepsy, autism, and Parkinson's disease. Understanding the molecular mechanism of positive modulators that enhance glutamatergic signaling will advance the development of more effective treatments for these disorders (Lynch, 2002; O'Neill et al., 2004; Black, 2005).

Understanding the molecular mechanism of allosteric modulation is contingent on understanding the fine details of AMPA receptor gating and, in particular, the decay of the AMPA receptor-mediated synaptic response, which may be terminated by two different, agonist-dependent mechanisms. When the exposure to glutamate is brief, AMPA receptor channels will close, and agonist may dissociate (deactivation), leaving receptors in an activatable state. On the other hand, prolonged exposure to glutamate causes channels to desensitize. In this case, receptors occupy a conformational state in which the bound agonist reduces the probability of channel opening. The channel must rearrange and recover before it can be activated again (Sun et al., 2002; Horning and Mayer, 2004; Robert et al., 2005; Armstrong et al., 2006; Weston et al., 2006; Zhang et al., 2008).

AMPA receptors are heterotetrameric membrane proteins composed of subunits GluA1 to GluA4 (Traynelis et al., 2010). Receptor functional heterogeneity is expanded through RNA splicing and RNA editing and through differential assembly with auxiliary accessory transmembrane proteins and cytoplasmic proteins that interact with the carboxyl terminus (Tomita, 2010). Each subunit is composed of four domains: an amino-terminal domain, a ligand-binding core or domain (LBC or LBD) to which both agonists and allosteric modulators bind, the membrane spanning domains (M1, M3, and M4) and a re-entrant pore loop (M2), and the cytoplasmic domain. It has been shown that the quaternary structure of the membrane spanning domain has 4-fold symmetry. In contrast, amino-terminal domain and LBC domains of the channel have two 2-fold axes of symmetry such that a dimer of dimers is created (Sobolevsky et al., 2009).

The LBC is composed of an upper lobe, domain 1, and a lower lobe, domain 2, which are brought together when agonist binds within the cleft formed between the domains (this structure may also be referred to as a "clamshell"). β-Strand hinges (clamshell hinges) that connect domains 1 and 2 impart stability upon the closed-cleft conformation. Once agonist is bound, the receptor may open and then desensitize, entailing a structural rearrangement of the interface between the paired LBCs of different subunits (Sun et al., 2002; Horning and Mayer, 2004; Quirk et al., 2004; Furukawa et al., 2005; Jin et al., 2005). On the other hand, upon brief exposure to glutamate, the receptor may deactivate by allowing the LBC cleft to reopen and glutamate to dissociate. Although time constants representing decays due to deactivation and desensitization can be determined experimentally, the structural relationship between these two processes is unclear.

Two classes of cognition-enhancing modulators for which there are structural data, the benzothiadiazides [e.g., cyclothiazide (CTZ)], and the pyrrolidinones [e.g., ampakine, 2*H*,3*H*,6a*H*-pyrrolidino(2,1–3′,2′)1,3-oxazino(6′,5′-5,4)benzo(*e*)1,4-dioxan-10-one (CX614)] are believed to favor the open-channel configuration by primarily slowing the onset of desensitization or rate of deactivation, respectively. CTZ predominantly modulates desensitization by preventing rearrangement at the dimer interface, thereby blocking entry into the desensitized state, with only a weak effect on deactivation of flip isoforms (Partin et al., 1996; Sun et al., 2002; Mitchell and Fleck, 2007). In contrast, CX614 slows desensitization with a profound effect on deactivation (Arai et al., 2000, 2002; Jin et al., 2005; Nagarajan et al., 2001).

Recent high-throughput screening assays have led to the development of a number of new positive allosteric modulators, including biarylsulfonamides (Ornstein et al., 2000; Miu et al., 2001), the series of amino indane sulfonamide derivatives (Ward and Harries, 2010; Ward et al., 2010b, 2011), and compounds based on the structure of *N*-[2-(4′-cyanobiphenyl-4-yl)propyl]propane-2-sulfonamide (LY404187) that then underwent "structure-based drug design" (Jamieson et al., 2010, 2011). Although excellent structural, and in some cases preclinical, information has been published on these compounds, less is understood about their biophysical mechanisms of action. Here, we describe structural and functional analyses of two new potent allosteric modulators of AMPA receptors, phenyl-1,4-bis-alkylsulfonamide (CMPDA), and phenyl-1,4-bis-carboxythiophene (CMPDB), and compare their actions on GluA2 with CTZ and CX614.

Materials and Methods

X-Ray Crystallography. Crystals of the iGluA2 flop extracellular domain were prepared using minor modifications of the methods described previously (Armstrong et al., 1998). The polypeptide sequence used for crystallization corresponds with that described as HS1S2H by Chen et al. (1998) and was refolded and crystallized as described by Armstrong and Gouaux (2000) and Chen et al. (1998) in the presence of glutamate by the hanging drop-vapor diffusion method using a precipitant solution containing 13 to 18% PEG 8000, 0.1 M $Zn(OAc)_2$, and 0.1 M sodium cacodylate at pH 6.5. Crystals were transferred into precipitant solutions containing 13 to 18% PEG 8000, 0.1 M zinc acetate, 0.1 M sodium cacodylate, pH 6.5, 3 mM CMPDA or CMPDB, and 3% DMSO. Crystals were incubated for 24 h and then flash-frozen in liquid nitrogen using cryoprotectant solution containing 30% PEG 8000, 20% glycerol, 0.1 M zinc acetate, and 0.1 M sodium cacodylate, pH 6.5. Diffraction data were collected on the Advanced Photon Source beamlines 17ID and 31ID and were integrated, merged, and scaled using the software package HKL2000 (HKL Research, Inc., Charlottesville, VA). Data scaling statistics are given in Table 1. Structures were solved using rigid body refinement of starting models derived originally from the Protein Data Bank 1LBC coordinates for CTZ structure in complex with the GluA2 LBC

TABLE 1

Scaling and refinement statistics

$R_{sym} = \Sigma|I - \langle I \rangle|/\Sigma I$, where I is the integrated intensity of a given reflection. The refinement residual, $R = \Sigma|F_{obs} - F_{calc}|/\Sigma F_{obs}$. Values for highest resolution bin are shown in parenthesis. R_{free}, calculated from 4546 observation test set for CMPDA and 4820 observation test set excluded for CMPDB.

	CMPDA	CMPDB
D_{max} (Å)	1.75	1.7
R_{sym}	0.067 (0.288)	0.055 (0.355)
$I/\sigma I$	22.3 (7.0)	25.8 (4.4)
Completeness (%)	99.8 (100.0)	98.5 (95.1)
Observations, unique (Total)	90,630 (735,725)	96,319 (596,873)
R (R_{free})	0.216 (0.247)	0.226 (0.2404)
RMSD		
Bonds (Å)	0.009	0.011
Angles (°)	1.482	1.554

RMSD, root-mean-square deviation from ideal values.

(Sun et al., 2002) against the diffraction data. Structures of CMPDA and CMPDB were fit to clear difference density maps using Afitt (Openeye, Inc., Santa Fe, NM) software. The models were iteratively refined using CNX (Accelyrs, Inc., San Diego, CA) and Refmac (Murshudov et al., 1999) software, with manual model building carried out using the program Coot (Emsley and Cowtan, 2004). Model refinement statistics are given in Table 1. Figures were generated from Protein Data Bank files using PyMOL (The PyMOL Molecular Graphics System, version 1.3; Schrödinger, Inc., Portland, OR). Molecular coordinates for CMPDA and CMPDB in complex with the GluA2 LBC have been deposited in the Protein Data Bank as 3RN8 and 3RNN, respectively.

Molecular Biology. Plasmids encoding cDNAs for the flip (i) and flop (o) variants of rat wild-type GluA2 were gifts of Dr. Peter Seeburg (University of Heidelberg, Heidelberg, Germany). The "WT GluA2" DNA plasmid contains a substitution of one residue within the pore, GluA2 $R_{607}Q$ (QuikChange II XL Site-Directed Mutagenesis Kit; Stratagene, La Jolla, CA), which recapitulates RNA editing of the pore, to facilitate electrophysiological studies. The receptors made from this mutant form homomers more efficiently, have greater conductances, and have an inwardly rectifying current-voltage relationship (Hume et al., 1991; Verdoorn et al., 1991).

HEK293 Cell Culture. Human embryonic kidney (HEK) 293 fibroblasts (American Type Culture Collection, Manassas, VA) were cultured as described previously (Cotton and Partin, 2000). Cells were cultured in Dulbecco's modified Eagle's medium supplemented with 10% fetal bovine serum (Gemini Bio-Products, Inc., Calabasas, CA), penicillin/streptomycin (100 U/ml each), and 1% GlutaMax-1 (both from Invitrogen, Carlsbad, CA). Cells were transiently transfected using FuGene 6 reagent (Roche Diagnostics, Indianapolis, IN) with GluA2 (GluA2i flip or GluA2o flop) cDNA and enhanced yellow fluorescent protein cDNA (1 and 0.2 μg/ 35-mm dish, respectively). For some experiments, 10 μM 2,3-dihydroxy-6-nitro-7-sulfamoylbenzo(*f*)quinoxaline was added after 18 to 24 h.

HEK293 Electrophysiology. Currents were recorded 24 to 72 h after transfection as described previously (Cotton and Partin, 2000). Outside-out membrane patches from transfected HEK293 cells were held under voltage-clamp at a holding potential of −60 mV using an Axopatch 200B amplifier (Molecular Devices, Sunnyvale, CA). Synapse software (version 3.6d) (Synergy Research, Inc., Bromma, Sweden) was used on a PowerPC Macintosh computer for trace analysis and data acquisition through an ITC-16 interface (HEKA, Lambrecht/Pfalz, Germany), which included control and timing of perfusion tubing movement by a piezoelectric device (Burleigh Instruments, Fishers, NY). Responses were filtered at 5 kHz and digitized at 10 to 500 μs/point. Electrodes of 2 to 5 MΩ were filled with 135 mM CsCl, 10 mM CsF, 10 mM HEPES, 5 mM cesium-BAPTA (Invitrogen, Carlsbad, CA), 1 mM $MgCl_2$, and 0.5 mM $CaCl_2$, pH 7.2, and 2 mM mM Na_2-ATP was added to the internal pipette solution immediately before recording each day. During recordings, cells were perfused continuously with extracellular control solution containing 20 mM sucrose, 145 mM NaCl, 5.4 mM KCl, 5 mM HEPES, 1 mM $MgCl_2$, 1.8 mM $CaCl_2$, and 0.01 mg/ml phenol red, pH 7.3. Currents were evoked with test solutions containing 10 mM glutamate. Control and test solutions were perfused through quartz θ tubing (Sutter Instrument Company, Novato, CA). The patch pipette tip was positioned in the control solution stream near the interface between the control and glutamate-containing streams. When modulators were used, they were added to both test and control solutions in the following concentrations: 100 μM CTZ, 100 μM CX614, and 10 μM CMPDA or CMPDB. Modulator stock solutions (10 mM) were dissolved in DMSO before dilution in extracellular solutions; final DMSO concentrations were 0.3 to 1%. When applying glutamate in the absence of modulator, after having perfused modulator through the tubing for a previous patch, we noticed that the steady-state current responses were not completely desensitized. This indicated that the modulators were sticking to the perfusion tubing and slowly leaching into the perfusion stream. We alleviated this problem by changing the tubing after using the modulator. On the other hand, this prevented us from collecting control and modulator data on the same patches. For this reason, and because of channel rundown, we do not report on differences in current amplitudes comparing control glutamate responses with those in modulator. Continuous solution flow was driven by a syringe pump (KD Scientific, New Hope, PA) at a rate of 0.2 ml/min; patches were preincubated in modulator for at least 2 min before switching into glutamate. No change in holding current was observed when the patches were initially brought into control solution containing modulators, indicating that the new modulators do not have intrinsic agonist properties. A piezoelectric device was used to drive rapid solution exchanges of 1 or 500 ms to measure channel deactivation or desensitization kinetics, respectively. Solution exchange rates were determined at the end of each experiment by measuring open-tip junction currents; for this purpose, the salts in the control solutions (no agonist) were diluted by 10%. Most of the decays of responses in the presence of modulator were best fit by the sum of two exponents. Data fit with a two-exponential function with both fast and slow components were combined into a weighted average time constant of exponential decay based on their respective amplitude contributions ($\%A_{Fast} \times \tau_{Fast} + \%A_{Slow} \times \tau_{Slow}$), where A is the amplitude of each time constant, τ. Data reported as mean ± S.E.M. were compared using analysis of variance with Dunnett's test for multiple comparisons within each receptor type to L-glutamate "control." Current traces and graphs were plotted using KaleidaGraph 3.6 (Synergy Software, Reading, PA).

Calcium Flux Assay. The ability of CMPDA and CMPDB to potentiate glutamate-evoked influx of calcium into HEK293 cells stably expressing human GluA2 (R607Q; Quirk and Nisenbaum, 2003) was evaluated using fluorometric imaging plate reader (FLIPR) technology (Molecular Devices). Confluent monolayers of stably transfected cells were prepared by delivering cells into 96-well plates at a density of approximately 60,000 cells/100 μl well and incubating plates at 37°C in 95% O_2/5% CO_2 overnight. The following day, the tissue culture medium in the wells was discarded, and 50 μl of Fluo3-acetoxymethyl ester dye (8 μM; Invitrogen) in Hanks' balanced salt solution buffer (Lonza Walkersville, Inc., Walkersville, MD) (plus 3.7 mM $CaCl_2$ and 20 mM HEPES) was added to each well. The plates were then incubated for 60 min at 25°C in the dark. After the incubation period, the Fluo3 dye was removed, and 50 μl of the Hanks' balanced salt solution buffer was added to each well, and the plate was placed into the FLIPR.

Test compounds were dissolved in 100% DMSO to yield 10 mM stock solutions. The stock solutions were diluted in buffer and tested in duplicate 10-point curves at concentrations of 0.0003 to 10.0 μM. The final DMSO concentration in the assay was 1.2%. Fluorometric readings were taken from each well after the addition of the compound alone (first addition) and after the addition of glutamate (100 μM) (second addition). Additional control wells contained glutamate (100 μM) alone and glutamate plus a maximal concentration of cyclothiazide (100 μM) used as a positive control compound. Compound effects were determined by subtracting the background fluorescence reading of each concentration of compound alone from the fluorescence reading obtained after the addition of each concentration of compound plus glutamate. These responses were then normalized to a signal window determined by the response to 100 μM cyclothiazide plus 100 μM glutamate (maximum response) and 100 μM glutamate alone (minimum response) and plotted. The data were then evaluated using nonlinear curve analyses, and the effective concentration yielding a 50% maximal response (EC_{50}) value was determined by fitting the data with a four-parameter logistic equation.

Mathematical Simulations of Currents. Simulations of currents under voltage clamp to an AMPA receptor model were performed using code originally written by John Clements (Benveniste et al., 1990), revised, and converted to an Igor Pro XOP (WaveMetrics, Lake Oswego, OR). Receptor state occupancies at each time point were determined numerically by calculating the change in each

state occupancy resulting from transitions into and out of each state according to first-order reaction rate kinetics as detailed in Benveniste et al. (1990). This was done iteratively at least 20 times per time point.

The model used in this study (Fig. 8A) is based on the activation and desensitization models for homomeric AMPA receptors of Robert and Howe, in which three open states of different conductance are possible, based on the binding of two, three, or four molecules of agonist (Rosenmund et al., 1998; Robert and Howe, 2003; Robert et al., 2005). This model has an added transition after agonist binding that represents the conformational change between the open and closed clamshell (cleft) states. The closed clamshell state precedes both the transition to the open state and the desensitized state. In addition, transition to desensitized states was also possible from the open state (Fig. 8A). Starting values for rate constants were taken from published values for GluA2 (Robert et al., 2005) and adjusted in the new model so as to yield similar values to the published peak and steady-state EC_{50} values and the time constants for the onset and recovery of desensitization. A full listing of the transitions for each model is presented in the Supplemental Material. The model was optimized to reflect experimental values for the flip isoform of GluR2. Flip and flop isoform-specific deactivation and desensitization kinetics have been simulated by others using a strategy of altering the rate of channel closing (k_{cl} or α) (Pei et al., 2007a,b). Although we tried to replicate that finding with the present model, we were unable to model the faster flop kinetics by simply increasing the rate of channel closing. With the present model, flip and flop differences were largely replicated by simply changing the rate of onset of desensitization by 10-fold. This apparent discrepancy exemplifies the model-dependence of kinetic analyses. Simulations and fitting and related analyses were run on a Macintosh MacBook Pro computer using Igor Pro 6.1 (WaveMetrics).

Gibbs Free Energy Calculations. The changes in stability resulting from the manipulation of rate constants for five basic receptor states (unbound; agonist bound, clamshell open; agonist bound, clamshell closed; open channel; and desensitized channel) were compared by converting forward and reverse reaction rates to Gibbs free energy of activation, $\Delta G^{\ddagger}$, according to the following equation: $\Delta G^{\ddagger} = RT \ln(k_B T/hk)$, where R is the universal gas constant, T is the absolute temperature (293 K), k_B is the Boltzmann constant, h is the Planck constant,and k is either the forward or reverse rate constant (Eyring, 1935; McNaught and Wilkinson, 1997). Changes in energy states are relative, with the unbound receptor state assumed to have a $\Delta G°$ value of 0 kcal/mol. In Fig. 9, the agonist-bound closed clamshell state is represented twice on successive rows to illustrate transitions from that state to either the open state or desensitized state. All chemicals were purchased from Sigma-Aldrich (St. Louis, MO) unless otherwise indicated.

Results

CMPDA and CMPDB Bind between Two Subunits at the Clamshell Hinges. Two positive allosteric modulators of AMPA receptors, CMPDA and CMPDB, were identified through a calcium influx screening assay of GluA2i and GluA2o receptors. Both compounds are derivatives of a biarylpropylsulfonamide series (Vandergriff et al., 2001; Shepherd et al., 2002) but are composed of a single central aryl ring with symmetrical *R*-groups. The alkylsulfonamide *R*-groups of CMPDA and the nitrile/thiophene *R*-groups of CMPDB extend above the plane of the aryl ring, whereas only the carboxyl groups of CMPDB extend below the plane of the aryl ring (Fig. 1). The ability of CMPDA and CMPDB to allosterically modulate GluA2i and GluA2o receptors stably transfected into HEK293 cells was assessed by measuring the glutamate-evoked influx of calcium using FLIPR technology. Potency estimates for the two compounds were determined by measuring the change in fluorescence each well after the addition of the compound alone at concentrations of 0.0003 to 10.0 μM and after the addition of glutamate (100 μM). The effects of CMPDA and CMPDB were determined by subtracting the background fluorescence reading of each concentration of compound alone from the fluorescence reading obtained after the addition of each concentration of compound plus glutamate. For each compound, the effects of each concentration were normalized to the response to 100 μM cyclothiazide plus 100 μM glutamate and plotted. Evaluation of the concentration-response plots revealed that the two compounds potently enhanced glutamate-induced calcium influx into HEK293 cells transfected with human GluA2i and GluA2o receptors (Supplemental Fig. 1). The potency for CMPDA at GluA2i receptors was EC_{50} = 45.4 ± 4.2 nM (mean ± S.E.M.; n = 4) and for GluA2o receptors was EC_{50} = 63.4 ± 5.6 nM (n = 4). The potency for CMPDB at GluA2i receptors was EC_{50} = 122.5 ± 12.9 nM (n = 2) and for GluA2o receptors was EC_{50} = 470.5 ± 3.7 nM (n = 2). Results showed that CMPDA was nearly equipotent at modulating

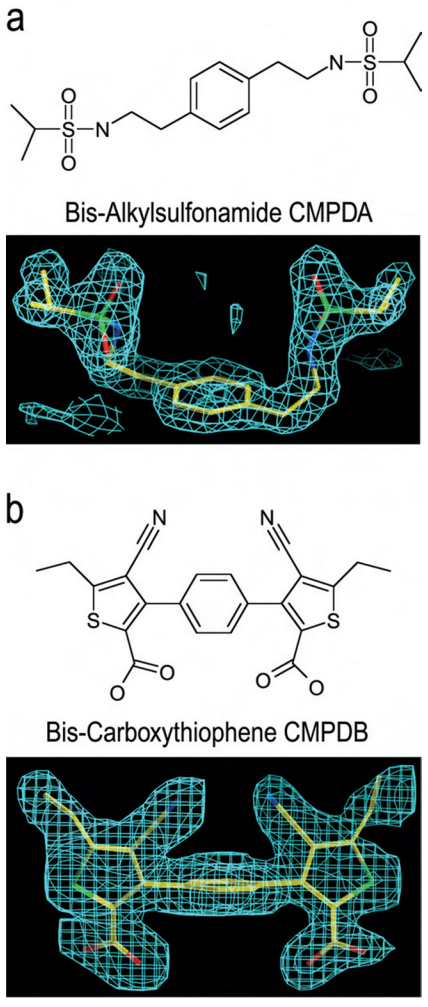

Fig. 1. Chemical structures (top) and omit electron density maps (bottom) of two positive allosteric modulators of AMPA receptors, a, bis-alkylsulfonamide 506091 (CMPDA); b, bis-carboxythiophene 2152080 (CMPDB). Omit density map for CMPDA (a) was calculated using $|F_o| - |F_c|$ coefficients, and view is shown perpendicular to the 2-fold axis. A simulated omit density map for CMPDB is shown (b).

the two isoforms of GluA2 receptors, whereas CMPDB displayed a modest preference for the flip splice variant.

High-resolution cocrystal structures of the isolated GluA2o LBC (HS1S2H) with L-glutamate and either CMPDA or CMPDB were solved (Table 1). Like the ampakine CX614 (Jin et al., 2005), a single molecule of CMPDA or CMPDB binds at the dimer interface, within a cleft situated near the interdomain hinges. The 2-fold symmetry of each compound is coincident with the 2-fold axes that relate subunits within the extracellular domain dimer (Fig. 2).

N1 and N2 of the alkylsulfonamide groups of CMPDA form hydrogen bonds with the main chain oxygens on residue Pro494 of both protomers. O_2 and O_4 form hydrogen bonds with the nitrogens on Gly731 for both protomers (Fig. 3, A and B). Residues Pro494 and Gly731 lie within the two interdomain β-strands of the AMPA receptor, making up the clamshell hinges (hinge 1, residues 494–498; hinge 2, residues 729–733). The two carboxyl groups of CMPDB also form hydrogen bonds with the interdomain hinges through the main chain nitrogen of residue Ser497 in protomer B and through water-mediated hydrogen bonds with the main chain oxygen of Phe495 of protomer B, main chain oxygen and nitrogen of Lys730 and main and side chains of Ser729 of protomers A and B (Fig. 3, C–E).

CMPDA and CMPDB Bind to the GluA2o Ligand Binding Core in a Space that Overlaps the CTZ and CX614 Binding Sites. Previous crystallographic studies have revealed that although CTZ and CX614 (and its parent compound, aniracetam) bind within the same region, at the dimer interface between two protomers, and interact with some of the same amino acid residues, they bind with different stoichiometries. CTZ binds with a modulator to protomer stoichiometry of 2:2, whereas CX614 (and aniracetam) has a 1:2 binding stoichiometry (Sun et al., 2002; Jin et al., 2003). Results from the current studies show that CMPDA and CMPDB also bind with a 1:2 stoichiometry similar to that of CX614. However, superposition of the crystal structures of the LBC bound to all four compounds clearly demonstrates that the set of residues that interact with CMPDA and CMPDB partially overlaps with those of both CTZ and CX614. The central phenyl rings of CMPDA and CMPDB are oriented similarly to the central aromatic ring of CX614, whereas the alkylsulfonamide and carboxythiophene groups partially overlap the space occupied by CTZ (Fig. 4).

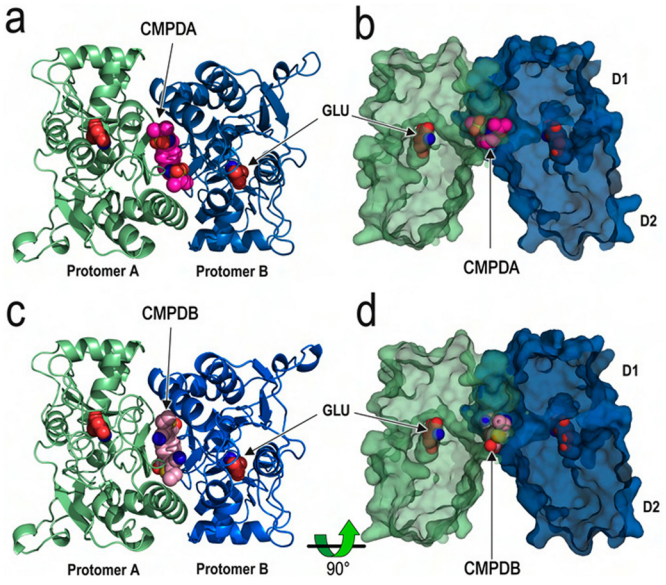

Fig. 2. CMPDA and CMPDB cocrystals with GluA2o HS1S2H and L-glutamate. a, one molecule of CMPDA (magenta CPK) binds within the dimer interface at the clamshell hinges. View looking down the 2-fold axis. Glutamate (GLU) is shown as red CPK. HS1S2H is shown. b, view of CMPDA perpendicular to the 2-fold axis, HS1S2H is shown in surface representation. c, One molecule of CMPDB (pink CPK) binds within the dimer interface at the clamshell hinges. View looking down the 2-fold axis. Glutamate is shown as red CPK. HS1S2H is shown. d, view of CMPDB perpendicular to the 2-fold axis, HS1S2H is shown in surface representation. D1 and D2, domains 1 and 2, respectively. Coordinates have been submitted to the Protein Data Bank as 3RNN and 3RN8, respectively.

CTZ and CX614 also have distinct effects on the deactivation and desensitization of AMPA receptors that are splice isoform-specific. For example, CTZ is more potent and efficacious in blocking desensitization of flip versus flop isoforms of AMPA receptors but only weakly modulates the deactivation of flip splice variants with little effect on flop-expressing receptors. In contrast to CTZ, CX614 is more efficacious at attenuating the desensitization of GluA2o receptors but also significantly slows deactivation in both GluA2i and GluA2o receptors (Arai et al., 2000; Jin et al., 2005; Mitchell and Fleck, 2007). Because the binding domains of CMPDA and CMPDB within the LBC are shared with both CTZ and CX614, we initially investigated whether the physical binding interactions could be used to predict the effects of CMPDA and CMPDB on the gating of GluA2i and GluA2o receptors.

A detailed analysis of the crystallographic structures of the four compounds (CTZ, CX614, CMPDA, and CMPDB) is necessary to assess the extent to which all four compounds interact with the same sets of residues but through differing types of interactions (Fig. 5). For example, Pro494 forms direct hydrogen bonds with CMPDA and CTZ, water-mediated bonds with CX614, and has a hydrophobic interaction with CMPDB; Ser497 forms water-mediated hydrogen bonds with CMPDB, water-mediated hydrogen bonds with CX614, and has a hydrophobic interaction with CMPDA. Ser729 forms a direct hydrogen bond with CTZ, water-mediated bonds with CMPDB and CX614, and has a hydrophobic interaction with CMPDA.

Most of the residues that interact with all four compounds reside in the hinge β-strands that connect the upper lobe (domain 1) to the lower lobe (domain 2) of the ligand-binding clamshell. The interaction between CMPDA or CMPDB and the hinges might suggest that they act to stabilize the closed-clamshell conformation of the protein, as proposed for CX614, resulting in the slowing of receptor deactivation. Stabilization of the clamshell closed conformation would enhance agonist-binding. This has been demonstrated for CX614, which enhances AMPA and fluorowillardiine binding and is in contrast to the effects of CTZ, which reduces agonist binding (Kessler and Arai, 2006). However, because CMPDA and CMPDB also have moieties that overlap with CTZ, modulation of deactivation might be superseded by effects on dimer interface stability. In addition, the crystal structure is static, representing a single snapshot of how CMPDA and CMPDB can interact with the ligand binding domain. It is difficult to predict the extent to which the efficacy of compound modulation may differ, depending on direct interactions with a residue versus making indirect, water-mediated contacts that may be perturbed by competing water molecules. We

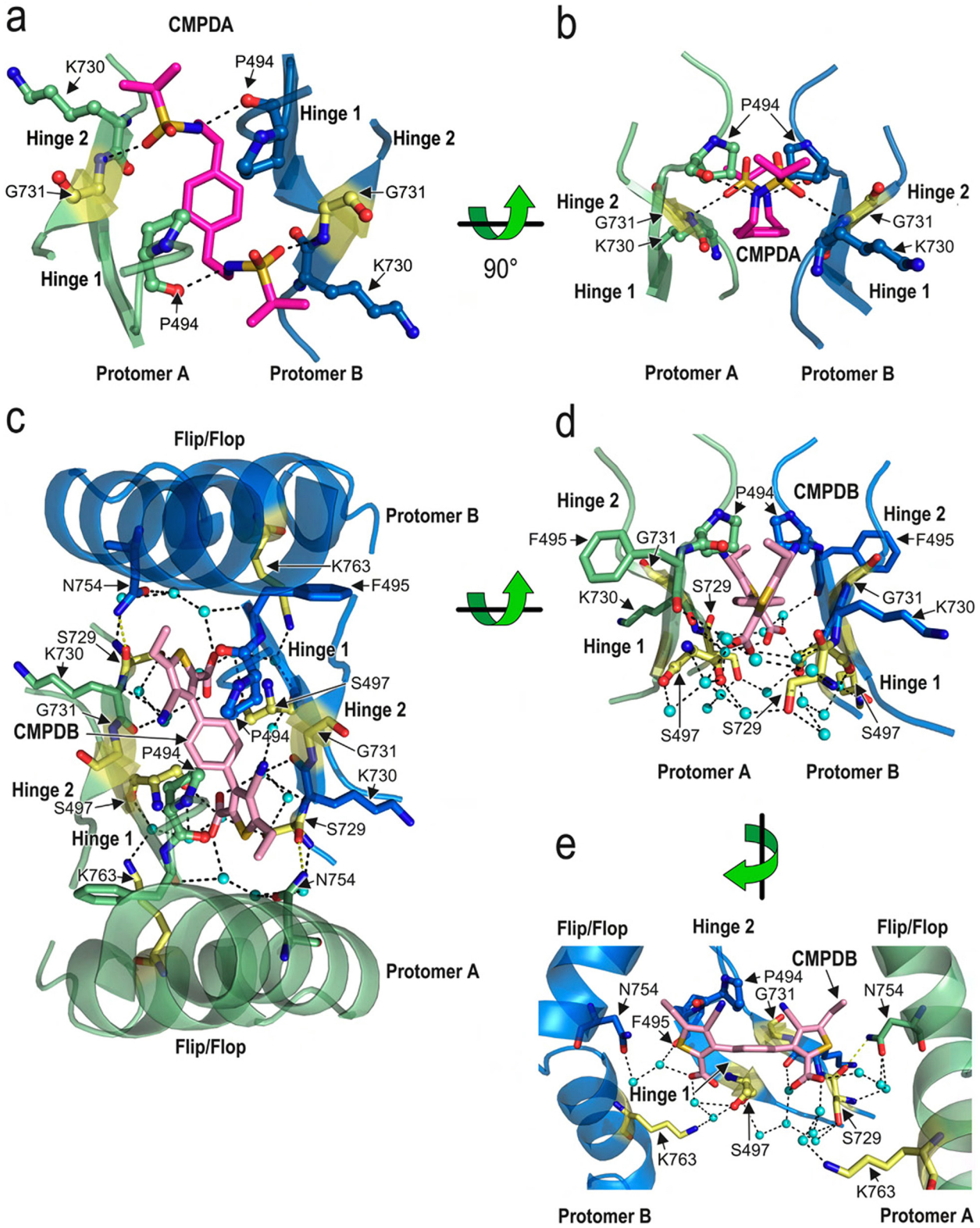

Fig. 3. Although both modulators bind at the dimer interface and hinges, they make different contacts with the receptor. a, top view of CMPDA (magenta stick) looking down the 2-fold axis of symmetry showing the relationship of CMPDA to the hinge regions of HS1S2H. b, side view of CMPDA rotated 90° around the *x*-axis from view a. c, top view of CMPDB (pink stick) showing the relationship of CMPDB to the flip/flop and hinge regions of S1SJ2. d, side view of CMPDB, rotated 90° around the *x*-axis from view c, omitting the flip/flop regions of protomers A and B for clarity. e, side view of CMPDB rotated 90° around the *y*-axis from view d, omitting the hinges of protomer B for clarity. Residues within 3.2 Å of CMPDA or CMPDB are shown in ball-and-stick representation with CPK colors and carbons colored according to protomer (green, A; blue, B). Yellow residues indicate sites of point mutations. Water molecules are shown as cyan spheres. Calculated hydrogen bonds are shown as black dashed lines. Yellow dashed lines represent the Asn754–Ser729 hydrogen bond.

therefore assessed the functional effects of CMPDA and CMPDB on the deactivation and desensitization processes of GluA2 flip and flop receptors and compared these effects with those of CTZ and CX614.

Functional Analysis of CMPDA and CMPDB Reveals Potent Modulation of Deactivation. To assess the effects of the modulators on channel activity, we measured responses evoked by ultrafast perfusion of glutamate to outside-out membrane patches from HEK293 cells expressing recombinant rat GluA2 AMPA receptors. Modulator effects on deactivation and desensitization were assessed using short (1-ms) and long (500-ms) pulses of glutamate (10 mM), respectively, in the presence and absence of concentrations of each of the four modulators that were predicted to be at "saturating" doses, based either on electrophysiological data (CX614 and CTZ) or FLIPR data (CMPDA and CMPDB).

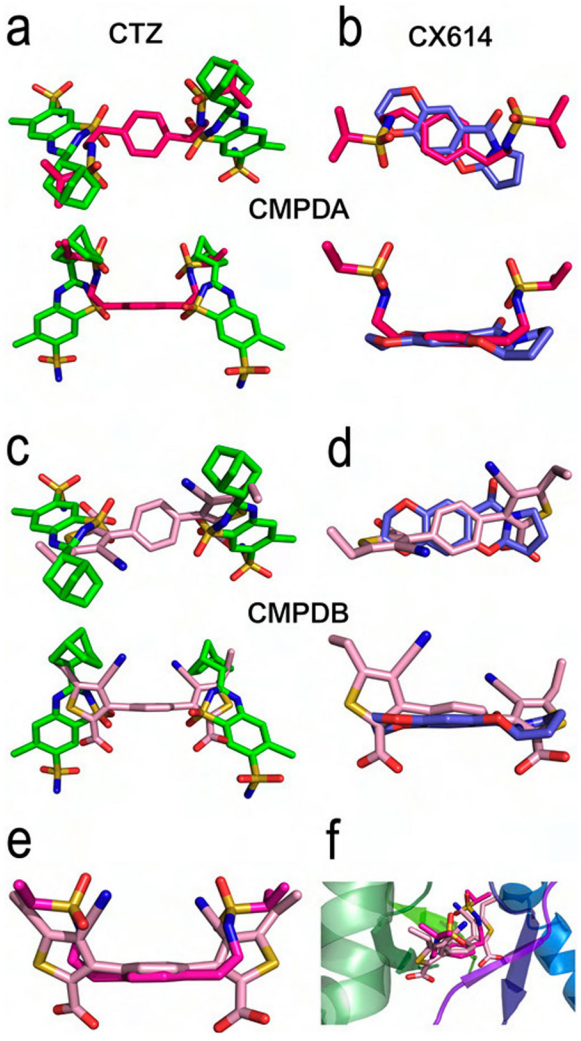

Fig. 4. CMPDA (magenta stick, a and b) and CMPDB (pink stick, c and d) share common groups with both classes of potentiators, CTZ (green stick, left) and ampakine, CX614 (slate blue stick, right). Aside from carbons, colors are shown in CPK. Top (top) and side (bottom) views of each overlay are provided. e, alignment of CMPDA and CMPDB. f, top view of same alignment in E rotated 90° around the *x*-axis illustrating the position of both compounds at the hinges and flip/flop regions. Protomer A (green) and protomer B (blue) are shown in ribbon format. The coordinates for CMPDA and CMPDB in complex with the HS1S2H LBC have been submitted. The coordinates used for CTZ and CX614 were 1LBC and 2AL4, respectively.

Both the flip (i) and flop (o) isoforms of rat GluA2 were tested to determine whether the modulators showed isoform selectivity.

Consistent with previous reports (Arai et al., 2000; Jin et al., 2005; Mitchell and Fleck, 2007), CX614 preferentially slowed deactivation of GluA2o receptors, whereas CTZ had no effect on deactivation of either GluA2i or GluA2o receptors (Fig. 6; Table 2). Similar to CX614, CMPDA slowed the rate of deactivation of GluA2o receptors approximately 2-fold but had no effect on GluA2i receptor deactivation. In contrast, CMPDB attenuated the rate of deactivation of both GluA2i and GluA2o receptors, although to differing degrees. The time constants of deactivation for GluA2i and GluA2o receptors were approximately 7- and 5-fold slower in the presence of CMPDB (Fig. 6; Table 2). Together, these results indicate that CMPDA was modestly flop-selective and CMPDB was generally more flip-selective in attenuating receptor deactivation.

As we have reported previously (Partin et al., 1995; Kessler et al., 2000; Quirk and Nisenbaum, 2003), CTZ eliminated desensitization of GluA2i receptors and significantly slowed the rate of desensitization of GluA2o receptors (Fig. 7 and Table 2). CX614 had similar effects on the extent of desensitization of GluA2i and GluA2o receptors such that the degree of desensitization (steady-state-to-peak) was approximately 65%. Results from the present study also showed that CMPDA robustly modulated receptor desensitization of both the flip and flop isoform of GluA2 receptors, virtually blocking the macroscopic onset of desensitization similar to the effects of CTZ on GluA2i receptors (Fig. 7; Table 2). CMPDB was as effective as CX614 on flip receptors (although it was not as effective as CTZ in blocking desensitization), but markedly less effective on flop receptors. The waveform of the decay was unusual in that onset of desensitization in the presence of CMPDB was similar to control, but the remaining large steady-state current for GluA2o reflect that the equilibrium desensitization differed. CMPDA and CX614 were nonselective for flip and flop isoforms, whereas CMPDB and CTZ exhibited a greater block of desensitization for the flip isoform.

Mathematical Modeling of Allosteric Modulation of AMPA Receptor Gating. Computer simulations of AMPA receptor gating have been used successfully to facilitate interpretation of complex electrophysiological data (Benveniste et al., 1990; Clements and Westbrook, 1991; Vyklicky et al., 1991; Raman and Trussell, 1992; Edmonds et al., 1995; Kessler et al., 1996; Partin et al., 1996; Mitchell and Fleck, 2007), including a widely accepted model that was recently developed and refined in a series of papers from the Howe laboratory (Robert and Howe, 2003; Robert et al., 2005; Zhang et al., 2008).

For the present studies, we were interested in understanding whether we could distinguish different mechanisms of modulation of receptor deactivation and desensitization. According to the Howe model, the macroscopic rate of deactivation would largely be determined by agonist affinity and/or by channel closing (α), whereas the macroscopic rate of desensitization would be governed by the onset and recovery from desensitization (δ, γ). Because crystal structures indicate that modulators of AMPA receptor desensitization may affect binding cleft stability (Jin et al., 2005), we modified the Howe model to explicitly account for agonist binding (k_f) and dissociation (k_{-f}), as well as clamshell closing (CC) and opening (CO) (Fig. 8A). This model allows for sequential, indepen-

dent agonist binding and cleft closing, which then leads to either channel opening or channel desensitization. We adjusted the parameters such that analysis of simulated currents yielded EC_{50} values at peak and steady state that were close to those of experimental data for GluA2 (Robert et al., 2005). For example, we increased the rate of β 2-fold and the rate of γ 3-fold. These adjustments also yielded time constants for the onset of and recovery from desensitization consistent with ours and other experimental data (Fig. 8, B and C), further validating the model.

Using simulations, we next wished to discern whether the effects of AMPA receptor modulators could be predicted by changes in isolated rate constants in our model. The manipulation of a single rate constant can influence the stability of receptor states in addition to the manipulated transition. For this reason, we have also included Gibbs free energy diagrams in Fig. 9. Because the binding of modulator is not explicitly modeled, the predicted results represent what would happen in the presence of a saturating concentration of modulator. The limits of solubility or availability of a modulator is a persistent technical issue for the current study; subsaturating concentrations result in partial effects on deactivation or desensitization. Thus, we are only sure of modulator potency when desensitization is totally blocked. Slowing the transition from the closed clamshell conformation to the open clamshell conformation by 100-fold ("Slow CO"; Fig. 9), produced a 2.4-fold slowing of in τ_{Deact} but also produced a slower low-amplitude decay in response to a sim-

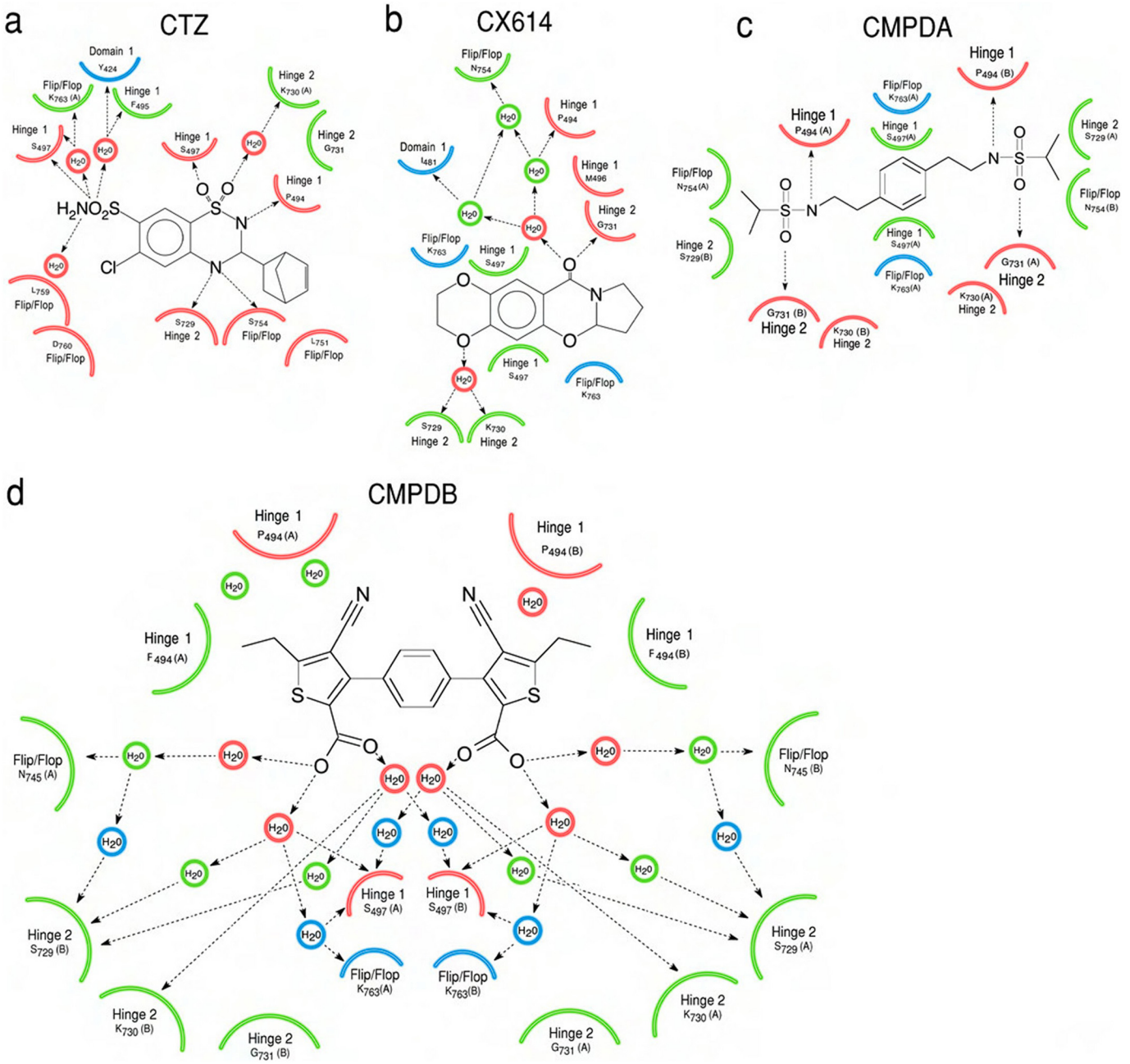

Fig. 5. Pharmacophores of CTZ (a), CX614 (b), CMPDA (c), and CMPDB (d) show different profiles of modulator binding. Water molecules and amino acid residues within 3.2 Å of each compound are defined by red semicircles (amino acids) or circles (water), between 3.3 and 4.9 Å (green), and greater than 5.0 Å from modulator (blue). Calculated hydrogen bonds are illustrated by black dashed arrows.

ulated 1-ms pulse of 10 mM glutamate (Fig. 9, top row). The rate of onset of desensitization could be examined by simulating a 500-ms pulse of 10 mM glutamate (Fig. 9, bottom row). This same manipulation of the CO rate constant also yielded a decrease in equilibrium desensitization, a phenomenon that was not observed with any of the modulators tested (Fig. 7).

Slowing the channel closing rate α by 20-fold caused a 4.4-fold decrease in τ_{Deact} and a 68% increase in the steady-state current, indicating partial block of desensitization without changing the rate of onset of desensitization ("Slow α," Fig. 9). These results are reminiscent of the effect of CMPDB on the flip isoform. Decreasing the rate of entry into the desensitized state δ by 100-fold had almost no effect on the decay of current after a 1-ms glutamate pulse but almost completely blocked desensitization ("Slow δ," Fig. 9). CTZ can block desensitization of the flip isoform (Fig. 7) whereas only weakly modulating deactivation (Fig. 6). These simulations suggest that this may occur by destabilizing the desensitized conformation.

Manipulation of a single rate constant could not reproduce experimental results for CMPDA on either AMPA receptor isoform. Thus, we proceeded with the simultaneous manipulation of two rate constants. Decreasing α by 20-fold and δ by 100-fold produced a 4.6-fold slowing of τ_{Deact} and complete block of desensitization (Slow α and δ, Fig. 9). However, similar results could be obtained by reducing the CO transition by 10-fold and the δ transition by 100-fold (Slow CO and δ, Fig. 9).

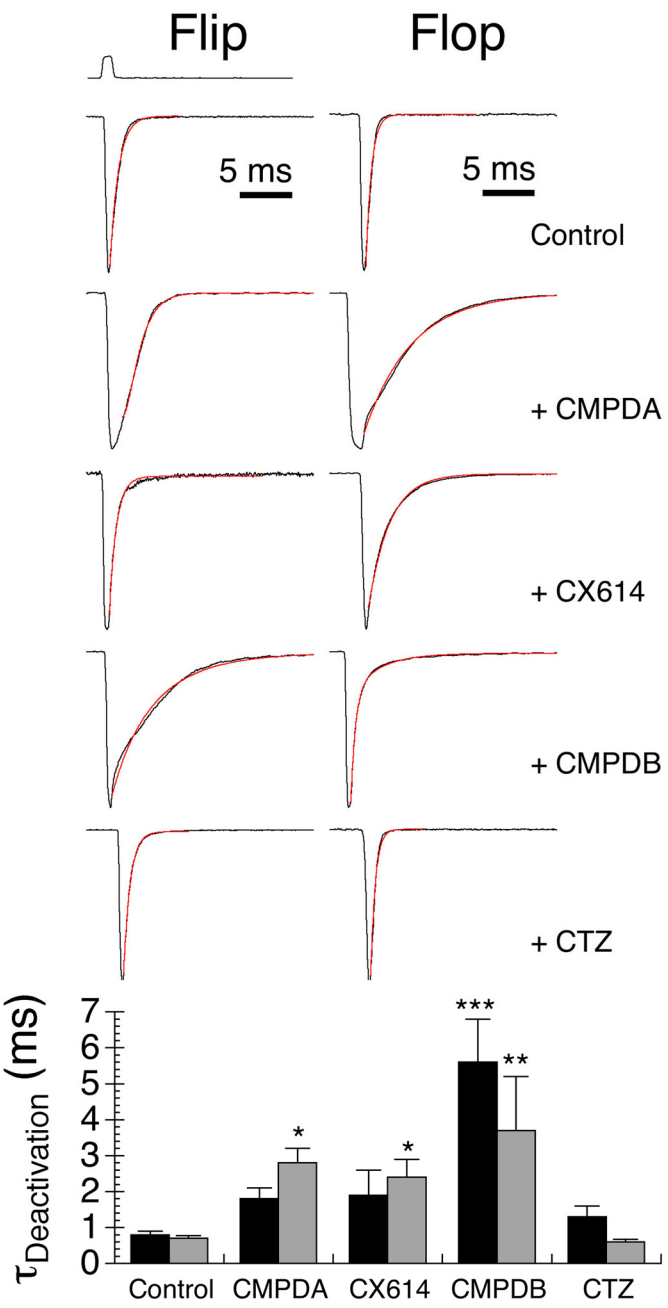

Fig. 6. CMPDA and CMPDB modulate deactivation of GluA2 flip and flop receptors. Representative traces for homomeric WT GluA2i (left) and GluA2o (right) receptors heterologously expressed in HEK293 cells exposed to 1 ms of glutamate alone or glutamate plus each of four modulators (to measure channel deactivation). The inverted trace (outward current) above the flip control trace is a representative open-tip junction potential, which reflects the rapidity of solution exchange. Fits to the sum of two exponentials are shown in red (see Table 2). Bar plot shows mean ± S.E.M. time constant of deactivation for flip (black bars) or flop (gray bar) isoforms of rat GluA2 receptors as described under *Materials and Methods*.

TABLE 2

Summary of mean modulation of WT GluA2 flip and flop

Summary of electrophysiology data for homomeric GluA2 WT receptors heterologously expressed in HEK293 cells exposed to glutamate alone or glutamate and each of four modulators. Data are reported as mean ± S.E.M. compared using analysis of variance with Dunnett's test for multiple comparisons within each receptor type to L-glutamate "control." Number of cells is given in parentheses. Data were fit with a two-exponential function, and both fast and slow components were combined into a weighted average based on their respective amplitude contributions ($\%A_{Fast} \times \tau_{Fast} + \%A_{Slow} \times \tau_{Slow}$), where A is the amplitude of each time constant.

	GluA2	
	Flip	Flop
10 mM Glutamate		
Weighted τ_{Des} (ms)	6.7 ± 0.4 (22)	1.6 ± 0.1 (22)
A_{fast} τ_{Des} (%)	51.8 ± 5.4	56.6 ± 4.5
%Des (1-ss/pk)	96.3 ± 0.8	97.1 ± 0.7
Weighted τ_{Deact} (ms)	0.8 ± 0.1 (21)	0.7 ± 0.07 (18)
A_{fast} τ_{Deact} (%)	55.4 ± 6.3	62.0 ± 6.2
10 μM CMPDA		
Weighted τ_{Des} (ms)	Non-Des (5)	Non-Des (12)
A_{fast} τ_{Des} (%)	Non-Des	Non-Des
%Des	8.0 ± 2.9***	6.1 ± 1.1***
Weighted τ_{Deact} (ms)	1.8 ± 0.3 (5)	2.8 ± 0.4* (12)
A_{fast} τ_{Deact} (%)	53.1 ± 10.4	45.6 ± 5.0
100 μM CX614		
Weighted τ_{Des} (ms)	7.25 ± 0.5 (8)[a]	121 ± 24.3*** (12)
A_{fast} τ_{Des} (%)	76.6 ± 3.4*	31.1 ± 5.2**
% Des	34.4 ± 5.5***	33.4 ± 2.1***
Weighted τ_{Deact} (ms)	1.9 ± 0.7 (10)	2.4 ± 0.5* (14)
A_{fast} τ_{Deact} (%)	77.0 ± 6.8	37.6 ± 4.5*
10 μM CMPDB		
Weighted τ_{Des} (ms)	49.0 ± 20.8* (7)	2.3 ± 0.2 (11)
A_{fast} τ_{Des} (%)	57.6 ± 4.8	92.1 ± 2.6***
%Des	34.4 ± 10.9***	81.5 ± 3.6***
Weighted τ_{Deact} (ms)	5.6 ± 1.2*** (7)	3.7 ± 1.5** (7)
A_{fast} τ_{Deact} (%)	43.9 ± 10.2	72.0 ± 13.9
100 μM CTZ		
Weighted τ_{Des} (ms)	Non-Des (8)	153 ± 12.3*** (8)
A_{fast} τ_{Des} (%)	Non-Des	11.9 ± 2.5***
%Des	4.3 ± 2.3***	67.3 ± 5.1***
Weighted τ_{deact} (ms)	1.3 ± 0.3 (8)	0.6 ± 0.07 (8)
A_{fast} τ_{deact} (%)	49.5 ± 12.1	59.1 ± 9.6

Non-Des, cells that did not desensitize in response to modulator.

[a] For WTGluA2i exposed to CX614, the initial phase of decay only was fit with a single exponential function due to "resensitization" as seen by the increasing inward current during the application of glutamate.

* $P < 0.05$.

** $P < 0.001$.

*** $P < 0.0001$.

Discussion

We describe here two new positive allosteric modulators of AMPA receptors: the bis-alykylsulfonamide CMPDA, and the bis-carboxythiophene CMPDB. Analysis of cocrystals of each compound with L-glutamate and the GluA2 flop ligand binding core reveal that both compounds have overlapping binding sites with CTZ and CX614, within the previously described modulator binding pocket located at the interdimer interface and the clamshell hinges. Our studies suggest that this pocket is a powerful target for drug discovery of compounds that modulate AMPA receptors and is a possible site of action for endogenous metabolites (Prescott et al., 2006).

An initial concern about developing modulators of AMPA receptors was the perceived need to increase their affinity and to improve their subunit and splice isoform selectivity. In

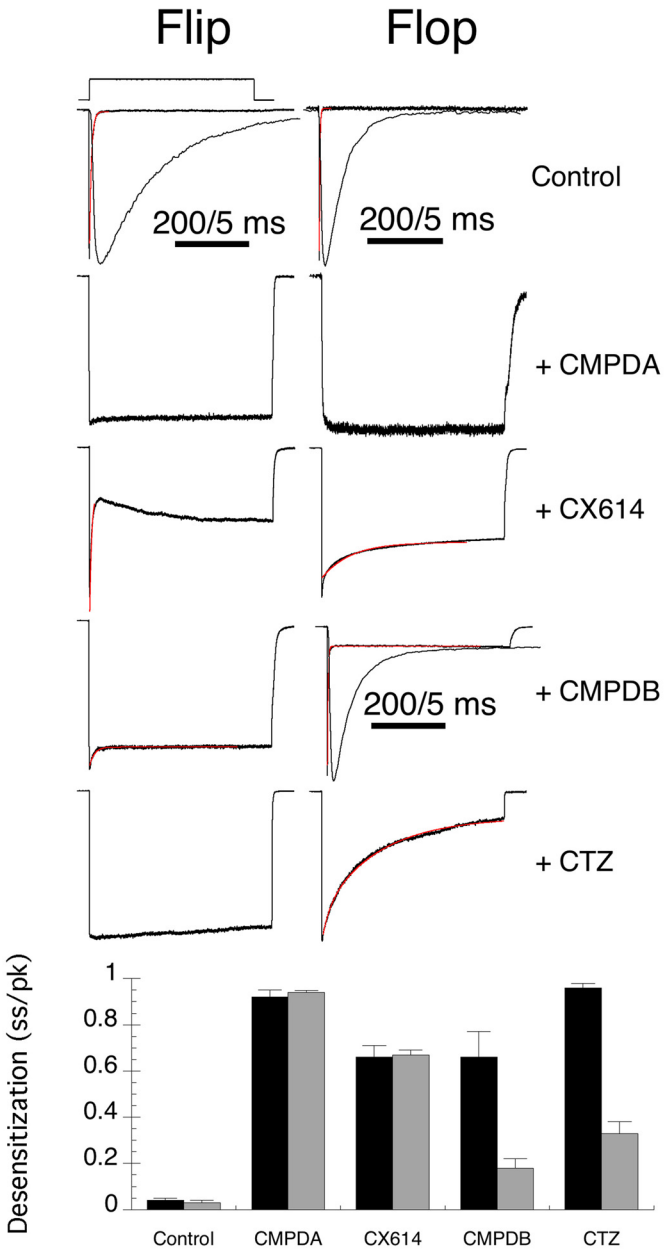

Fig. 7. CMPDA and CMPDB modulate desensitization of GluA2 flip and flop receptors. Representative traces for homomeric WT GluA2i (left) and GluA2o (right) receptors heterologously expressed in HEK293 cells exposed to 500 ms of glutamate alone or glutamate plus each of four modulators (desensitization protocol). The inverted trace above the flip control trace is a representative open-tip junction potential indicating when glutamate was applied. Fits to the sum of two exponentials are shown in red and represent the onset of desensitization kinetics (see Table 2). Note that the calibration bar represents 200 ms for all. In addition, an expanded trace for three is shown for which the calibration bar represents 5 ms. Bar plot shows mean ± S.E.M. of the steady-state divided by peak current amplitudes (ss/pk) for flip (black bars) or flop (gray bars) GluA2 receptors.

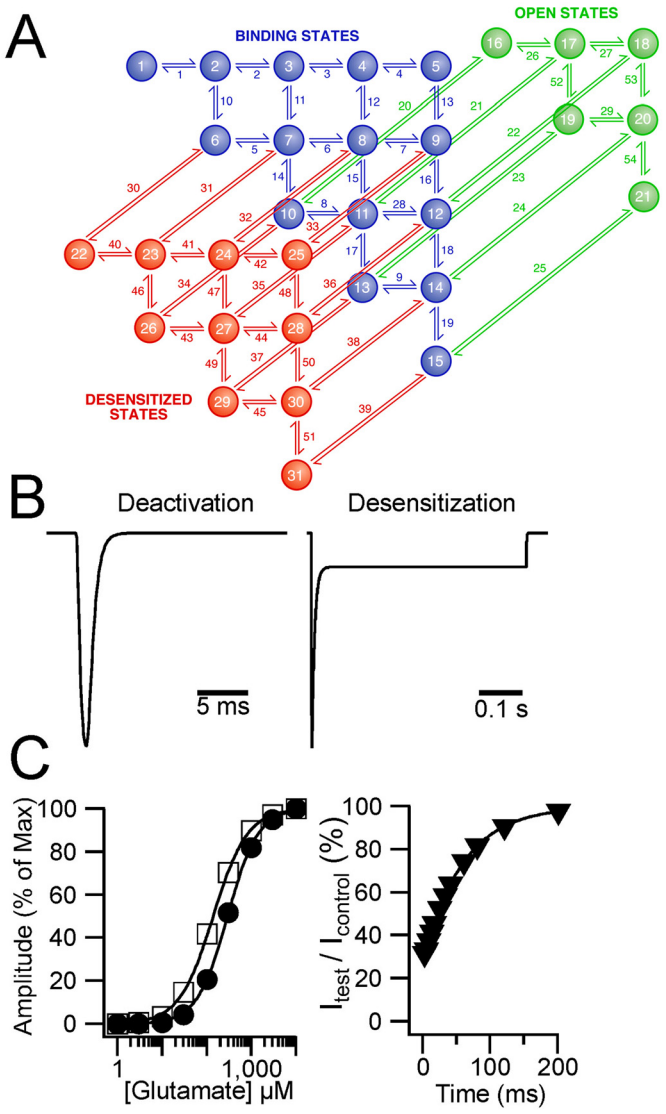

Fig. 8. Simulations of AMPA receptor gating. a, state diagram describing a model for AMPA receptor gating in which the CC and CO are explicitly modeled. Blue circles represent closed states, green circles represent open states, and red circles represent desensitized states. Sequential glutamate binding is represented by transitions from left to right (k_f and k_{-f}) and can occur in closed open and desensitized states. Conformational transitions in the clamshell are represented by vertical transitions. Two clamshell closures are required before the transition to the open state (β and α transitions). A complete description of the states and rates of transitions is reported in the Supplemental Data (Table S1). B, simulated responses to 1- and 500-ms pulses of 10 mM glutamate. A single exponential fit of the decays results in a τ_{Deact} = 0.7 ms and τ_{Des} = 6.2 ms, similar to GluA2i experimental data. C, simulated dose response for peak (●) and steady-state (□) currents in response to 1 to 10,000 μM pulses of glutamate (left); simulated recovery from desensitization in a paired pulse paradigm (right). Fits to the simulated data yield EC_{50}peak = 292 μM, EC_{50}ss = 139 μM, and a $\tau_{recovery}$ = 59 ms. These fits are close approximations to experimental data presented in this article and to data that have been reported previously (Zhang et al., 2008).

this regard, CMPDA and CMPDB provide important new insight. CMPDA and CMPDB effectively block desensitization at lower concentrations than some of the modulators described previously (Figs. 6 and 7), indicating that the site is amenable to the development of new, therapeutically relevant compounds.

It has been proposed that the allosteric modulatory site can be delineated into five overlapping subsites at the dimer interface between subunits (Ptak et al., 2009). The central subsite, A, lies parallel to the axis of symmetry between the protomers and is occupied by the planar rings of aniracetam, CX614, and the biaryl compounds. Hinge residues (connecting domain 1 and domain 2 of one protomer), particularly Pro497, Ser497, and Ser729 form hydrogen bonds with these compounds and through these interactions are believed to stabilize closed clamshell conformations (Jin et al., 2003). Subsite B, or B′ on the opposing protomer, is an exposed, hydrophilic pocket formed by residues Tyr424, Phe495, Ser497, Lys763, and Ser729, whereas subsite C (C′) is a deep, hydrophobic pocket lined by residues Ile481, Lys493, and Leu751. CMPDA fully blocks desensitization in both flip and flop isoforms and binds directly to subsites A and C. Residues that form subsite C play an important role in dimer interface stability and may be critical for dimer interactions that permit receptor desensitization (Sun et al., 2002; Horning and Mayer, 2004). CMPDB, which binds to subsites A and C but also has extensive interactions in subsite B, shows surprising isoform selectivity for blocking desensitization that is not predicted from its binding characteristics (Fig. 7). This may suggest that modulator binding in subsite B can influence isoform selectivity through direct interaction or by destabilizing interactions through subsite C. Consistent with this, CTZ preferentially blocks desensitization of the flip isoform through the interaction of its N4 substituent with the serine/asparagine site on helix J (Sun et al., 2002; Ptak et al., 2009). Although Ser/Asn750 lies between the B and C subsites, the asparagine limits access to the C subsite. The occupancy of CMPDA and CMPDB may also be compared with that of some of the newly described positive allosteric modulators, such as compound **7a** that was characterized in Ward et al., 2011. Similar to CMPD A, **7a** has a phenyl moiety that occupies site A and a trifluoromethyl group that interacts with the hydrophobic pocket of subsite C and therefore would be predicted to impede desensitization as its related compound, **9a**, was shown to do (Ward et al., 2011). Additional insight has been garnered from the "hybridization" studies of

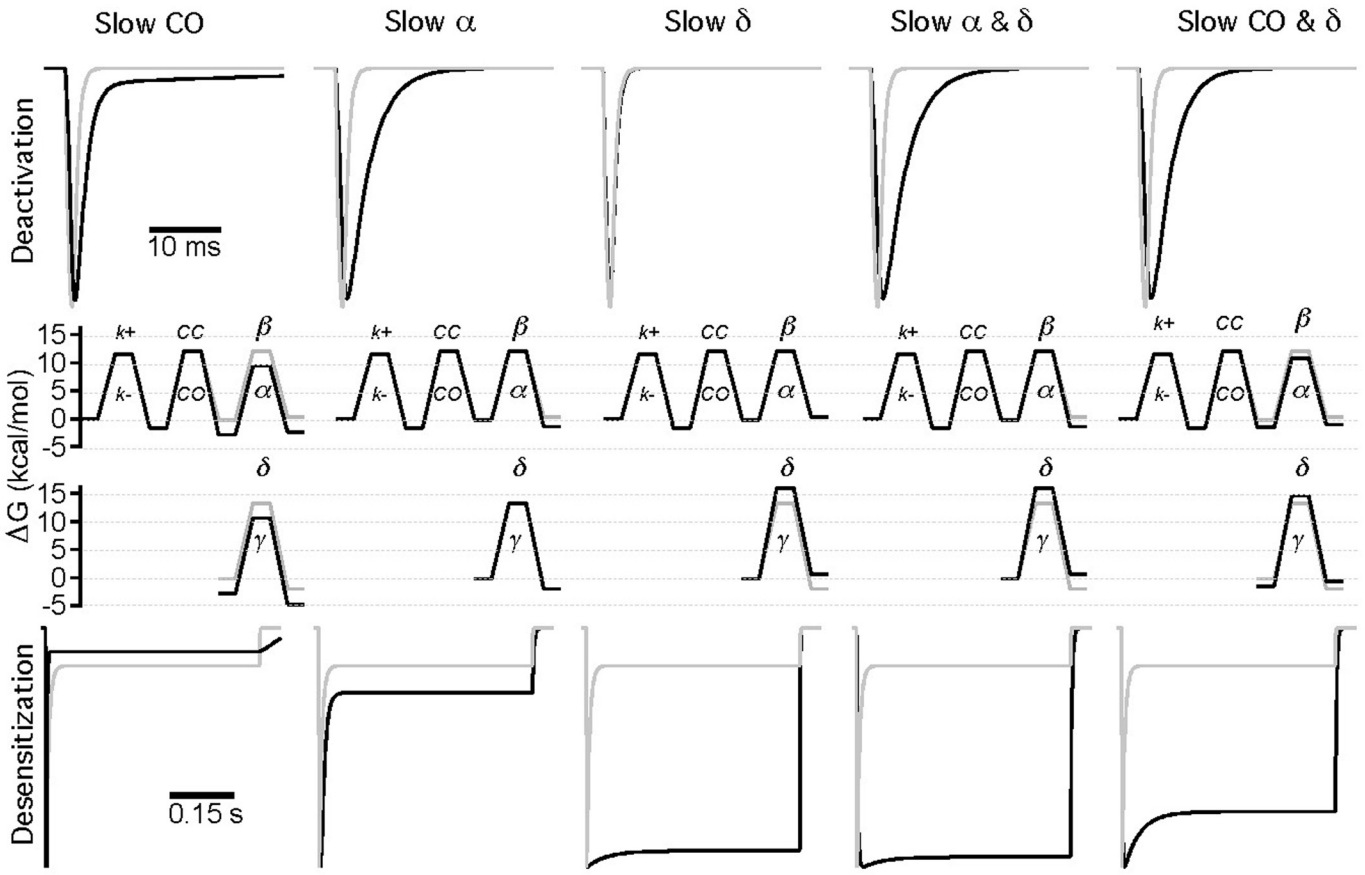

Fig. 9. Changes in rate constants in the model predict changes in the kinetics of deactivation and desensitization observed by modulators. Simulations of GluA2 currents under voltage-clamp in response to 10 mM glutamate for either a 1-ms pulse to observe deactivation kinetics (top) or a 500-ms pulse to observe desensitization kinetics (bottom). Simulated GluA2 currents under control conditions (no modulator) are represented by gray traces. Potential effects of modulator (black traces) are segregated by column and have been simulated by slowing either the CO, α, or δ transitions in isolation or in combination. The middle row shows how changes in the rate constants influence the stability of various receptor states, as measured by estimated changes in Gibb's free energy (Δ*G*). The troughs from left to right represent the following: the unbound receptor, the agonist bound receptor in the open clamshell state, the agonist bound receptor in the closed clamshell state, and the open channel. The lower middle row repeats the trough found above it and shows the transition to the agonist bound desensitized state (states not shown are identical with those shown above). Results indicate that CTZ can be simulated by slowing δ, CMPDB can be simulated by slowing α, and CMPDA can be simulated by slowing α and δ or CO and δ.

Jamieson et al. (2010, 2011), which demonstrate the chemical synthesis of a molecule that hybridizes structural features from LY404187 and compound **1** derived from a high-throughput screen. Although the biophysical attributes of the hybridized structure have not yet been published, functional screens indicate that a degree of flexibility between the moieties that occupy the central subsite and the two pockets (A and C) is critical to potent modulation (Jamieson et al., 2011).

Cocrystals of the flip and flop interface of the GluA2 LBC with agonist are not markedly different (Ahmed et al., 2009), suggesting that the modulator-bound crystal structure may not be the dominant conformer for one or both isoforms. To pursue this, we performed a site-directed mutational analysis of residues in GluA2i and GluA2o that were predicted to contribute to the binding site based upon their proximity to the modulator in the crystal structure. Mutations of residues found closest to each of the different modulators did, in fact, have the greatest affect on the ability of the modulator to block receptor desensitization (A. M. Weeks, K. M. Partin, and M. Benveniste, manuscript in preparation).

The functional implications of the selectivity of CMPDB may be significant. Regarding the selectivity, one of the concerns about using AMPA receptor positive modulators clinically is our insufficient understanding of how the balance of inhibition and excitation in neuronal circuitry is changed by enhancing AMPA receptor activity at excitatory synapses, which belong to either excitatory or inhibitory postsynaptic neurons. For instance, the CA1 region of the hippocampus contains pyramidal neurons that are excitatory but also receive input from inhibitory interneurons that are themselves activated by excitatory input. Effects of ampakines 6-(piperidin-1-ylcarbonyl)quinoxaline (CX516) and 2,3-dihydro-1,4-benzodioxin-7-yl-(1-piperidyl)methanone (CX546) (which are slightly flop-selective) on excitation have been shown to outweigh their effects on inhibition, whereas CTZ seems to have a similar effect on both pyramidal cells and interneurons (Xia et al., 2005). It is noteworthy that principal neurons express AMPA receptors composed predominantly of flip isoforms, whereas interneurons express AMPA receptors with a substantial flop component (Geiger et al., 1995). Thus, CMPDB would be predicted to enhance the excitatory component of principal neurons, although not effectively modulating the AMPA receptors on inhibitory cells, whereas CMPDA would affect both types of cells equally. This isoform selectivity, together with the potent modulation by CMPDB of deactivation rather than desensitization, makes it an ideal candidate for further drug discovery efforts. Future studies in an in vitro brain slice preparation using CMPDB could provide important new information relevant to the development of the AMPA receptor complex for therapeutic benefit.

Insight into the Molecular Mechanisms of Allosteric Modulation Using Modeling. Figs. 6 and 7 clearly show differential effects of modulators on deactivation and desensitization, which can also be isoform-specific. However, without using single-channel electrophysiology techniques, we can only measure macroscopic rates of modulation. Our interpretation of the macroscopic data is confounded by the fact that changes in desensitization rates can influence the macroscopic rate of deactivation, and changes in deactivation rates can affect macroscopic rates of desensitization. Furthermore, the structural determinants that alter deactivation (the cleft and clamshell hinges) spatially overlap with the structural determinants of desensitization (the dimer interface).

The goal of kinetic modeling is to test different mechanisms of action. In many cases, this also provides a way to use macroscopic data to support or refute mechanisms with microscopic rates and transitions, in the absence and presence of drugs. The unique features of our kinetic model over the well established Howe model (Robert and Howe, 2003; Robert et al., 2005) are that it explicitly incorporates clamshell opening and closing and allows for ligand-binding transitions between open states (we could think of no valid reason why channel-opening prevents binding access to other independent subunits). The simulated data presented suggest that these alterations did not invalidate the Howe model but rather allowed us to specifically investigate how opening and closing of the clamshell influenced deactivation and desensitization kinetics. Although these four modulators all bind to the interface between LBC protomers, could we reproduce their effects on desensitization and deactivation by manipulating the same transitions for each drug? In fact, interpretation of the modeling data suggests that the drugs are mechanistically quite different depending on how they interact with each of the five subsites. To a first approximation, CTZ modulation can be simulated by slowing δ, consistent with its full occupancy of subsite C, residues of which play an important role in hydrogen and salt bridge interactions, which are broken to allow receptor desensitization (Horning and Mayer, 2004). CMPDB can be simulated by slowing α, consistent with its occupancy of subsites A and B, through which CMPDB interacts with hinge domain side chains and backbone moieties. CMPDA can be simulated by slowing α and δ or CO and δ.

A second goal was to model explicitly whether modulators of deactivation act primarily on the rate of channel closing (α) (Vyklicky et al., 1991; Partin et al., 1996; Suppiramaniam et al., 2001) or clamshell reopening (CO) (Jin et al., 2005). Unfortunately, the model did not distinguish between direct effects on clamshell stability through interactions with the hinges (slowing of CO) or allosteric effects on channel gating through dimer interactions (slowing of α). We might expect that slowing CO and δ might be a more likely mechanism for modulator action because the slowing CO and δ are associated through their common closed clamshell state, whereas affecting α and δ are more likely two independent processes. Yet, aniracetam has been shown to increase single-channel open times in native AMPA receptors in cultured neurons, indicating that two separate effects of modulator are possible (Vyklicky et al., 1991). Modulation by CX614 has also been simulated by slowing α using the original Howe model (Robert and Howe, 2003; Robert et al., 2005; Mitchell and Fleck, 2007). Aniracetam and CX614 bind primarily within the A subsite of the allosteric modulatory site at the dimer interface and have a strong effect on deactivation kinetics but a weaker effect on desensitization (Figs. 6 and 7). This evidence, together with the modeling data (Fig. 9), suggests that the hinge region coinciding with subsite A may modulate deactivation by slowing α. Another way to look at this issue is to ask whether stabilizing the closed clamshell conformation could solely explain efficacious block of desensitization and a slowing of deactivation. However, our modeling data suggest that only destabilization of the desensitized state can easily produce nondesensitizing currents (Fig. 9) and that

stabilizing the agonist bound closed cleft state by slowing CO is not sufficient to reproduce our findings with the various modulators (Fig. 7).

Future experiments directed at understanding the molecular mechanism of existing allosteric modulators, as well as the discovery and development of new modulators, will also have to take into account the important contributions that accessory subunits make toward determining the efficacy and potency of modulation (Tomita et al., 2006). In general, transmembrane AMPA receptor regulatory proteins such as stargazin shift modulator efficacy dose response curves leftward, significantly increasing the activity of the AMPA receptors they associate with, and thereby enhancing the postsynaptic responses elicited.

Acknowledgments

We thank John Gieser for help in the production of this manuscript. We thank Dr. Gary Rogers, Cortex Pharmaceuticals, Inc., for the kind gift of CX614.

Authorship Contributions

Participated in research design: Timm, Benveniste, Weeks, Nisenbaum, and Partin.

Conducted experiments: Timm, Benveniste, Weeks, and Partin.

Contributed new reagents or analytic tools: Benveniste and Nisenbaum.

Performed data analysis: Timm, Benveniste, Weeks, Nisenbaum, and Partin.

Wrote or contributed to the writing of the manuscript: Timm, Benveniste, Weeks, Nisenbaum, and Partin.

Other: Benveniste and Partin acquired funding for the research.

References

Ahmed AH, Wang Q, Sondermann H, and Oswald RE (2009) Structure of the S1S2 glutamate binding domain of GLuR3. *Proteins* **75:**628–637.

Arai A, Kessler M, Ambros-Ingerson J, Quan A, Yigiter E, Rogers G, and Lynch G (1996a) Effects of a centrally active benzoylpyrrolidine drug on AMPA receptor kinetics. *Neuroscience* **75:**573–585.

Arai A, Kessler M, Rogers G, and Lynch G (1996b) Effects of a memory-enhancing drug on DL-alpha-amino-3-hydroxy-5-methyl-4-isoxazolepropionic acid receptor currents and synaptic transmission in hippocampus. *J Pharmacol Exp Ther* **278:** 627–638.

Arai AC, Kessler M, Rogers G, and Lynch G (2000) Effects of the potent ampakine CX614 on hippocampal and recombinant AMPA receptors: interactions with cyclothiazide and GYKI 52466. *Mol Pharmacol* **58:**802–813.

Arai AC, Xia YF, Rogers G, Lynch G, and Kessler M (2002) Benzamide-type AMPA receptor modulators form two subfamilies with distinct modes of action. *J Pharmacol Exp Ther* **303:**1075–1085.

Armstrong N and Gouaux E (2000) Mechanisms for activation and antagonism of an AMPA-sensitive glutamate receptor: crystal structures of the GluR2 ligand binding core. *Neuron* **28:**165–181.

Armstrong N, Jasti J, Beich-Frandsen M, and Gouaux E (2006) Measurement of conformational changes accompanying desensitization in an ionotropic glutamate receptor. *Cell* **127:**85–97.

Armstrong N, Sun Y, Chen GQ, and Gouaux E (1998) Structure of a glutamate-receptor ligand-binding core in complex with kainate. *Nature* **395:**913–917.

Benveniste M, Clements J, Vyklický L Jr, and Mayer ML (1990) A kinetic analysis of the modulation of *N*-methyl-D-aspartic acid receptors by glycine in mouse cultured hippocampal neurones. *J Physiol* **428:**333–357.

Black MD (2005) Therapeutic potential of positive AMPA modulators and their relationship to AMPA receptor subunits. A review of preclinical data. *Psychopharmacology* (*Berl*) **179:**154–163.

Chen GQ, Sun Y, Jin R, and Gouaux E. (1998) Probing the ligand binding domain of the GluR2 receptor by proteolysis and deletion mutagenesis defines domain boundaries and yields a crystallizable construct. *Protein Sci* **7:**2623–2630.

Clements JD and Westbrook GL (1991) Activation kinetics reveal the number of glutamate and glycine binding sites on the N-methyl-D-aspartate receptor. *Neuron* **7:**605–613.

Cotton JL and Partin KM (2000) The contributions of GluR2 to allosteric modulation of AMPA receptors. *Neuropharmacology* **39:**21–31.

Edmonds B, Gibb AJ, and Colquhoun D (1995) Mechanisms of activation of glutamate receptors and the time course of excitatory synaptic currents. *Annu Rev Physiol* **57**:495–519.

Emsley P and Cowtan K (2004) Coot: model-building tools for molecular graphics. *Acta Crystallogr D Biol Crystallogr* **60:**2126–2132.

Eyring H (1935) The activated complex in chemical reactions. *J Chem Phys* **3:**107–119.

Furukawa H, Singh SK, Mancusso R, and Gouaux E (2005) Subunit arrangement and function in NMDA receptors. *Nature* **438:**185–192.

Geiger JR, Melcher T, Koh DS, Sakmann B, Seeburg PH, Jonas P, and Monyer H (1995) Relative abundance of subunit mRNAs determines gating and Ca^{2+} permeability of AMPA receptors in principle neurons and interneurons in rat CNS. *Neuron* **15:**193–204.

Goff DC, Leahy L, Berman I, Posever T, Herz L, Leon AC, Johnson SA, and Lynch G (2001) A placebo-controlled pilot study of the ampakine CX516 added to clozapine in schizophrenia. *J Clin Psychopharmacol* **21:**484–487.

Horning MS and Mayer ML (2004) Regulation of AMPA receptor gating by ligand binding core dimers. *Neuron* **41:**379–388.

Hume RI, Dingledine R, and Heinemann SF (1991) Identification of a site in glutamate receptor subunits that controls calcium permeability. *Science* **253:**1028–1031.

Ingvar M, Ambros-Ingerson J, Davis M, Granger R, Kessler M, Rogers GA, Schehr RS, and Lynch G (1997) Enhancement by an Ampakine of memory encoding in humans. *Experimental Neurology* **146:**553–559.

Jamieson C, Campbell RA, Cumming IA, Gillen KJ, Gillespie J, Kazemier B, Kiczun M, Lamont Y, Lyons AJ, Maclean JK, et al. (2010) A novel series of positive modulators of the AMPA receptor: structure-based lead optimization. *Bioorg Med Chem Lett* **20:**6072–6075.

Jamieson C, Maclean JK, Brown CI, Campbell RA, Gillen KJ, Gillespie J, Kazemier B, Kiczun M, Lamont Y, Lyons AJ, et al. (2011) Structure based evolution of a novel series of positive modulators of the AMPA receptor. *Bioorg Med Chem Lett* **21:**805–811.

Jin R, Banke TG, Mayer ML, Traynelis SF, and Gouaux E (2003) Structural basis for partial agonist action at ionotropic glutamate receptors. *Nature Neuroscience* **6:**803–810.

Jin R, Clark S, Weeks AM, Dudman JT, Gouaux E, and Partin KM. Mechanism of positive allosteric modulators acting on AMPA receptors. *J Neurosci* 25(39):9027–9036, 2005.

Kessler M, Arai A, Quan A, and Lynch G (1996) Effect of cyclothiazide on binding properties of AMPA-type glutamate receptors: lack of competition between cyclothiazide and GYKI 52466. *Mol Pharmacol* **49:**123–131.

Kessler M and Arai AC (2006) Use of [3H]fluorowillardiine to study properties of AMPA receptor allosteric modulators. *Brain Res* **1076:**25–41.

Kessler M, Rogers G, and Arai A (2000) The norbornenyl moiety of cyclothiazide determines the preference for flip-flop variants of AMPA receptor subunits. *Neurosci Lett* **287:**161–165.

Lynch G (2002) Memory enhancement: the search for mechanism-based drugs. *Nat Neurosci* **5 (Suppl):**1035–1038.

McNaught AD and Wilkinson A (1997) *IUPAC Compendium of Chemical Terminology: the "Gold Book."* Blackwell Scientific Publications, Oxford, UK.

Mitchell NA and Fleck MW (2007) Targeting AMPA receptor gating processes with allosteric modulators and mutations. *Biophys J* **92:**2392–2402.

Miu P, Jarvie KR, Radhakrishnan V, Gates MR, Ogden A, Ornstein PL, Zarrinmayeh H, Ho K, Peters D, Grabell J, et al. (2001) Novel AMPA receptor potentiators LY392098 and LY404187: effects on recombinant human AMPA receptors in vitro. *Neuropharmacology* **40:**976–983.

Murshudov GN, Vagin AA, Lebedev A, Wilson KS, and Dodson EJ (1999) Efficient anisotropic refinement of macromolecular structures using FFT. *Acta Crystallogr D Biol Crystallogr* **55:**247–255.

Nagarajan N, Quast C, Boxall AR, Shahid M, and Rosenmund C (2001) Mechanism and impact of allosteric AMPA receptor modulation by the ampakine CX546. *Neuropharmacology* **41:**650–663.

O'Neill MJ, Bleakman D, Zimmerman DM, and Nisenbaum ES (2004) AMPA receptor potentiators for the treatment of CNS disorders. *Curr Drug Targets CNS Neurol Disord* **3:**181–194.

Ornstein PL, Zimmerman DM, Arnold MB, Bleisch TJ, Cantrell B, Simon R, Zarrinmayeh H, Baker SR, Gates M, Tizzano JP, et al. (2000) Biarylpropylsulfonamides as novel, potent potentiators of 2-amino-3- (5-methyl-3-hydroxyisoxazol-4-yl)- propanoic acid (AMPA) receptors. *J Med Chem* **43:**4354–4358.

Partin KM, Bowie D, and Mayer ML (1995) Structural determinants of allosteric regulation in alternatively spliced AMPA receptors. *Neuron* **14:**833–843.

Partin KM, Fleck MW, and Mayer ML (1996) AMPA receptor flip/flop mutants affecting deactivation, desensitization, and modulation by cyclothiazide, aniracetam, and thiocyanate. *J Neurosci* **16:**6634–6647.

Pei W, Huang Z, and Niu L (2007a) GluR3 flip and flop: differences in channel opening kinetics. *Biochemistry* **46:**2027–2036.

Pei W, Ritz M, McCarthy M, Huang Z, and Niu L (2007b) Receptor occupancy and channel-opening kinetics: a study of GLUR1 L497Y AMPA receptor. *J Biol Chem* **282:**22731–22736.

Prescott C, Weeks AM, Staley KJ, and Partin KM (2006) Kynurenic acid has a dual action on AMPA receptor responses. *Neurosci Lett* **402:**108–112.

Ptak CP, Ahmed AH, and Oswald RE (2009) Probing the allosteric modulator binding site of GluR2 with thiazide derivatives. *Biochemistry* **48:**8594–8602.

Quirk JC and Nisenbaum ES (2003) Multiple molecular determinants for allosteric modulation of alternatively spliced AMPA receptors. *Journal of Neuroscience* **23:**10953–10962.

Quirk JC, Siuda ER, and Nisenbaum ES (2004) Molecular determinants responsible for differences in desensitization kinetics of AMPA receptor splice variants. *J Neurosci* **24:**11416–11420.

Raman IM and Trussell LO (1992) The kinetics of the response to glutamate and kainate in neurons of the avian cochlear nucleus. *Neuron* **9:**173–186.

Robert A, Armstrong N, Gouaux JE, and Howe JR (2005) AMPA receptor binding cleft mutations that alter affinity, efficacy, and recovery from desensitization. *J Neurosci* **25:**3752–3762.

Robert A and Howe JR (2003) How AMPA receptor desensitization depends on receptor occupancy. *J Neurosci* **23:**847–858.
Rosenmund C, Stern-Bach Y, and Stevens CF (1998) The tetrameric structure of a glutamate receptor channel. *Science* **280:**1596–1599.
Shepherd TA, Aikins JA, Bleakman D, Cantrell BE, Rearick JP, Simon RL, Smith EC, Stephenson GA, Zimmerman DM, Mandelzys A, et al. (2002) Design and synthesis of a novel series of 1,2-disubstituted cyclopentanes as small, potent potentiators of 2-amino-3-(3-hydroxy-5-methyl-isoxazol-4-yl)propanoic acid (AMPA) receptors. *J Med Chem* **45:**2101–2111.
Sobolevsky AI, Rosconi MP, and Gouaux E (2009) X-ray structure, symmetry and mechanism of an AMPA-subtype glutamate receptor. *Nature* **462:**745–756.
Stäubli U, Perez Y, Xu FB, Rogers G, Ingvar M, Stone-Elander S, and Lynch G (1994a) Centrally active modulators of glutamate receptors facilitate the induction of long-term potentiation in vivo. *Proc Natl Acad Sci USA* **91:**11158–11162.
Staubli U, Rogers G, and Lynch G (1994b) Facilitation of glutamate receptors enhances memory. *Proc Natl Acad Sci USA* **91:**777–781.
Sun Y, Olson R, Horning M, Armstrong N, Mayer M, and Gouaux E (2002) Mechanism of glutamate receptor desensitization. *Nature* **417:**245–253.
Suppiramaniam V, Bahr BA, Sinnarajah S, Owens K, Rogers G, Yilma S, and Vodyanoy V (2001) Member of the Ampakine class of memory enhancers prolongs the single channel open time of reconstituted AMPA receptors. *Synapse* **40:**154–158.
Tomita S (2010) Regulation of ionotropic glutamate receptors by their auxiliary subunits. *Physiology* **25:**41–49.
Tomita S, Sekiguchi M, Wada K, Nicoll RA, and Bredt DS (2006) Stargazin controls the pharmacology of AMPA receptor potentiators. *Proc Natl Acad Sci USA* **103:**10064–10067.
Traynelis SF, Wollmuth LP, McBain CJ, Menniti FS, Vance KM, Ogden KK, Hansen KB, Yuan H, Myers SJ, and Dingledine R (2010) Glutamate receptor ion channels: structure, regulation, and function. *Pharmacol Rev* **62:**405–496.
Vandergriff J, Huff K, Bond A, and Lodge D (2001) Potentiation of responses to AMPA on central neurones by LY392098 and LY404187 in vivo. *Neuropharmacology* **40:**1003–1009.
Verdoorn TA, Burnashev N, Monyer H, Seeburg PH, and Sakmann B (1991) Structural determinants of ion flow through recombinant glutamate receptor channels. *Science* **252:**1715–1718.
Vyklicky L Jr, Patneau DK, and Mayer ML (1991) Modulation of excitatory synaptic transmission by drugs that reduce desensitization at AMPA/kainate receptors. *Neuron* **7:**971–984.
Ward SE, Bax BD, and Harries M (2010a) Challenges for and current status of research into positive modulators of AMPA receptors. *Br J Pharmacol* **160:**181–190.
Ward SE and Harries M (2010) Recent advances in the discovery of selective AMPA receptor positive allosteric modulators. *Curr Med Chem* **17:**3503–3513.
Ward SE, Harries M, Aldegheri L, Andreotti D, Ballantine S, Bax BD, Harris AJ, Harker AJ, Lund J, Melarange R, et al. (2010b) Discovery of *N*-[(2*S*)-5-(6-fluoro-3-pyridinyl)-2,3-dihydro-1*H*-inden-2-yl]-2-propanesulfonamide, a novel clinical AMPA receptor positive modulator. *J Med Chem* **53:**5801–5812.
Ward SE, Harries M, Aldegheri L, Austin NE, Ballantine S, Ballini E, Bradley DM, Bax BD, Clarke BP, Harris AJ, Harrison SA, Melarange RA, Mookherjee C, Mosley J, Dal Negro G, Oliosi B, Smith KJ, Thewlis KM, Woollard PM, and Yusaf SP (2011) Integration of lead optimization with crystallography for a membrane-bound ion channel target: discovery of a new class of AMPA receptor positive allosteric modulators. *J Med Chem* **54:**78–94.
Weston MC, Schuck P, Ghosal A, Rosenmund C, and Mayer ML. Conformational restriction blocks glutamate receptor desensitization. *Nat Struct Mol Biol* 13(12): 1120–1127, 2006.
Xia YF, Kessler M, and Arai AC (2005) Positive alpha-amino-3-hydroxy-5-methyl-4-isoxazolepropionic acid (AMPA) receptor modulators have different impact on synaptic transmission in the thalamus and hippocampus. *J Pharmacol Exp Ther* **313:**277–285.
Yamada KA and Rothman SM (1992) Diazoxide blocks glutamate desensitization and prolongs excitatory postsynaptic currents in rat hippocampal neurons. *J Physiol* **458:**409–423.
Zhang W, Cho Y, Lolis E, and Howe JR (2008) Structural and single-channel results indicate that the rates of ligand binding domain closing and opening directly impact AMPA receptor gating. *J Neurosci* **28:**932–943.

Address correspondence to: Dr. Kathryn M. Partin, Department of Biomedical Sciences, Colorado State University, Fort Collins, CO 80523-1617. E-mail: kathy.partin@colostate.edu